

Stability assessment of indocyanine green within dextran-coated mesocapsules by absorbance spectroscopy

Mohammad A. Yaseen

Rice University
Department of Bioengineering
MS-142, P.O. Box 1892
Houston, Texas 77251-1892

Jie Yu

Michael S. Wong

Rice University
Department of Chemical and Biomolecular Engineering
MS-362, P.O. Box 1892
Houston, Texas 77251-1892

Bahman Anvari

University of California, Riverside
Department of Bioengineering
900 University Avenue
A-227 Bourns Hall
Riverside, California 92521

Abstract. The biocompatibility and high absorption in the near IR range of indocyanine green (ICG) have made it a suitable candidate chromophore for optical imaging and laser-mediated therapy of superficial tumors. However, its clinical efficacy remains limited by factors such as rapid circulation kinetics, lack of target specificity, and molecular instability. Such drawbacks motivated us to encapsulate ICG into carrier particles to improve target specificity and retention time. We use absorbance spectroscopy to investigate the effects of encapsulating ICG within dextran-coated capsules. The mesocapsules (MCs) containing ICG are synthesized using a previously reported charge-assembly technique. Both freely dissolved ICG and ICG-MCs are prepared with ICG concentrations of either 50 or 10 $\mu\text{g}/\text{ml}$. Samples are exposed either to a broadband light source or incubated at 3, 23, or 40°C. Absorbance spectra are recorded at various time points up to 96 h. At the lower concentration of 10 $\mu\text{g}/\text{ml}$, ICG within MCs experiences less light-induced degradation. The MC system also protects ICG from thermal degradation at all tested temperatures. The polymer-salt aggregate core of the MCs hinders the mobility of ICG molecules. The MC system shields ICG from vibrational and translational agitation as well as molecular changes such as fragmentation. © 2007 Society of Photo-Optical Instrumentation Engineers. [DOI: 10.1117/1.2821423]

Keywords: cancer; drug delivery; optical imaging; photodynamic therapy; photothermal therapy; tumor.

Paper 07161R received May 8, 2007; revised manuscript received Jul. 18, 2007; accepted for publication Aug. 9, 2007; published online Dec. 27, 2007.

1 Introduction

Indocyanine green (ICG) is a tricyanocyanine dye that absorbs and fluoresces in the near-IR (NIR) wavelength region^{1,2} (650 to 850 nm). It is used extensively in clinical settings to measure cardiac output and plasma volume, image choroidal structure, and assess liver function.^{3,4} The minimal toxicity and vascular retention of ICG have motivated investigations into its utility for diagnostic purposes and a variety of therapeutic applications including photodynamic therapy, tissue welding, and photothermal therapy.⁵⁻¹⁴ As water and most intrinsic biomolecules within tissue do not absorb strongly within the NIR range,¹⁵ optical targeting of exogenously administered ICG may enable the selective treatment of deeper tissue structures. Our previous studies have demonstrated that ICG is a useful exogenous chromophore for laser-mediated destruction of blood vessels within rabbit earlobes as a model system for hypervascular lesions.¹⁶

After a bolus injection, the concentration of ICG within the bloodstream drops at an exponential rate, with a half time (τ)

ranging between 2 and 4 min. ICG binds readily to plasma proteins and is rapidly excreted to bile.^{1,17} The inability to localize freely dissolved ICG to a desired target and its relatively short retention time within the target limits its potential for diagnostic and therapeutic applications. Moreover, ICG effectiveness is hindered by its molecular instability, which causes^{18,19} its optical properties to vary with factors such as concentration, temperature, solvent medium, and pH.

The absorbance spectrum of ICG varies considerably with concentration. ICG molecules in solution remain in monomeric form at concentrations below approximately 400 $\mu\text{g}/\text{ml}$, and the absorbance spectrum shows a peak between 780 and 810 nm, depending on the solvent medium.¹⁸ At higher concentrations, ICG forms dimers and oligomers, resulting in a new, lower absorbance peak between 680 and 730 nm, again dependent on the solvent medium. At even higher concentrations (greater than 1.2 mg/ml), ICG is prone to J-aggregation, a process in which the molecules self-organize over time into a highly aggregated, thread-like arrangement. The presence of J-aggregates results^{20,21} in increased absorbance at a new peak of $\lambda_J = 893$ nm.

Address all correspondence to Bahman Anvari, Ph.D., Professor, Department of Bioengineering, University of California, Riverside, 900 University Ave., A-227 Bourns Hall, Riverside, CA 92521; Tel: 951-827-5726; Fax: 951-827-6416; E-mail: anvari@engr.ucr.edu

ICG is known to undergo a variety of physicochemical transformations in aqueous media. It degrades over time through the formation of leucoforms, a molecular species with less conjugation, resulting in diminished absorbance in the IR range, discoloration, and a shift in peak absorbance.^{18,20,21} The degradation process occurs more readily in response to light exposure or elevated temperatures.²²

In an effort to overcome the drawbacks faced with freely dissolved ICG, researchers are currently investigating techniques to encapsulate ICG into nanometer-sized carrier particles.^{23–25} Encapsulation within these nanoparticles has the potential to modulate the circulation kinetics of drugs, and by functionalizing the particle surface, therapeutic agents could be localized to targeted locations in the body. Researchers have reported on the use of ICG encapsulated in oil-water emulsion particles as a chromophore for photothermal heating.^{23,24} Other investigators have encapsulated ICG at lower concentrations (1 $\mu\text{g}/\text{ml}$) in biocompatible poly (*D,L*-lactide-co-glycolide) (PLGA) nanoparticles for fluorescence contrast imaging.²⁵

We have previously reported^{26,27} on the synthesis and characterization of nanoparticle-assembled capsules (NACs) containing ICG. With particle diameters less than 1000 nm, the NACs contain a polymer-matrix core consisting of positively charged polymer molecules, poly-(allylamine hydrochloride) (PAH), bridged by negatively charged multivalent phosphate salt molecules. A coating of 13-nm silica nanoparticles surrounded the core. Through charge interactions, ICG molecules are embedded within the polymer-salt matrix core and through the capsule surface. When compared to other encapsulation methods, the NACs offer the advantage of easy synthesis process, size controllability, and encapsulation efficiency.

Incorporating ICG into the NAC delivery capsules gives rise to a potentially localizable photothermal absorbing system suitable for laser heating of abnormal tissue structures such as superficial tumors. In this study, we incorporate ICG into a modified version of the NAC capsule system in which the silica nanoparticle coating is replaced by dextran polymer, allowing for increased biocompatibility and functionalization.²⁸ Our capsule diameters range between 400 and 800 nm, smaller than the diameter range of microcapsules (>1000 nm) and yet larger than the range of particles conventionally referred to as nanoparticles (<100 nm). Consequently, we employ the term “mesocapsule” (MC) to refer to these dextran capsules to reflect their intermediate diameter range. The dextran outer coating and polymer-salt matrix core in our MC system limit the ability of the ICG molecules to interact with plasma proteins, and therefore could potentially slow down the excretion kinetics from the vasculature. We envision that the MC system can be used to accumulate ICG at the targeted location. On subsequent exposure to high pH or temperature, the MCs can be disassembled, liberating ICG within the microenvironment of the target. We focus on determining how encapsulating ICG within MCs can influence the sensitivity of ICG to temperature and light exposure. Specifically, absorbance measurements were recorded on (1) ICG released from disassembled MCs and (2) freely dissolved ICG to assess how encapsulation affected the absorbance spectrum. The degradation kinetics of both systems at different

temperatures and when exposed to intense broadband light and different temperatures were evaluated.

2 Materials and Methods

2.1 MC Preparation

ICG was purchased in powder form under the product name Cardiogreen from Sigma. Stock solutions of 500 $\mu\text{g}/\text{ml}$ were prepared by dissolving the powder form into sterile, triple-distilled water, covered with foil, and refrigerated at 3 °C to minimize degradation.

ICG-containing MCs were prepared using a simple three-step process. The initial step involved the development of a spherical polymer-salt matrix by lightly mixing 0.5 ml poly-(allylamine hydrochloride) (PAH, 2 mg/ml in deionized H₂O, 4 °C) with 3 ml disodium phosphate (Na₂HPO₄, 0.01 M, pH=7.4, 4 °C) for 10 s in a 15-ml centrifuge tube. Through ionic crosslinking, a cationic polymer-salt aggregate was formed between the positively charged PAH polymers and the HPO₄²⁻ anions. The ratio of total negative charge of the added salt to the total positive charge of the polymer, denoted as the *R* ratio, was 6, satisfying the necessary conditions for aggregate formation.^{26,27}

The second step followed immediately after aggregate formation. The aggregate suspension was mixed with aqueous ICG solution (0.5 mg/ml, 1.5 ml) for 30 s. By electrostatic attraction and hydrophobic interaction, the negatively charged ICG molecules penetrated into the aggregates. By adding a more dilute solution of ICG (0.1 mg/ml, 1.5 ml) in, a batch of MCs containing less ICG was also prepared for the light exposure studies. These MCs with less ICG were compared with a diluted preparation of ICG solution. In the final step, an additional 0.5 ml of dextran polymer (40 kDa, purchased from Aldrich, 2 mg/ml in H₂O) was added to the mixture and mixed for 30 s. The dextran molecules formed a coating around the surface of the aggregate through electrostatic interaction and H-bonding. The capsules were allowed to age for 2 h, at which point they were centrifuged at 7000 rpm for 30 min and resuspended in 6.5 ml phosphate-buffered saline (PBS) by sonication. The process was repeated twice to remove excess precursors. The resultant MCs remained suspended in PBS, with pH close to physiological levels in blood (pH=7.4), for the duration of the experiments.

For comparison with the MCs, ICG aqueous solution was made by diluting the 500 $\mu\text{g}/\text{ml}$ ICG stock solution with sterile PBS. A concentration of 50 $\mu\text{g}/\text{ml}$ was chosen to match the ICG concentration contained in the MC suspensions. More dilute ICG solution was made to match the ICG concentration in the less concentrated MC preparations by further diluting down to 10 $\mu\text{g}/\text{ml}$.

2.2 Absorbance Spectroscopy

Absorbance measurements were taken from 400 to 900 nm using a spectrophotometer (Shimadzu UV-2401PC) equipped with a tungsten excitation lamp. For each absorbance reading, 500 μl of sample was extracted and placed in an Eppendorf tube. Immediately before taking the absorbance measurement, 50 μl of 1 M NaOH was added to each sample to increase the pH. Increasing the pH served two purposes. Earlier experiments revealed that, at a higher pH (pH>11), the MCs

lost their integrity and ICG was liberated back into solution. Disassembling the capsules eliminated the effect of Mie scattering by the submicrometer-diameter MCs. Additionally, it was found that the nonlinear relationship between ICG concentration and its absorbance spectrum, which results from ICG's tendency to form molecular aggregates at higher concentrations, was eliminated over a wide concentration range at higher pH (unpublished results). After adding NaOH, 500 μl of the sample was removed and further diluted in 2.5 ml of PBS in a disposable cuvette. PBS was used as a reference for all absorbance measurements. Stability of ICG at high pH was also assessed. Preparations of ICG in PBS at high pH (pH > 11) and concentrations ranging from 5 to 50 $\mu\text{g/ml}$ were stored in the dark at room temperature. Absorbance profiles of these samples were recorded at $t=0, 20, 40,$ and 60 min. No differences in the absorbance profiles were observed up to 1 h after preparation. By taking a standard curve, the relationship between peak absorbance value and ICG concentration was found to be linear over the range of concentrations used in this study, from 1.25 to 25 $\mu\text{g/ml}$.

2.3 Calculation of Encapsulation Efficiency

To measure the encapsulation efficiency (η) of ICG within the MCs, a standard absorbance profile was created from the peak absorbance values of several samples of freshly dissolved ICG in PBS at different concentrations. The mass of ICG encapsulated within the MCs was determined by measuring the absorbance value of supernatants and disintegrated MCs and relating the measurements to their corresponding ICG concentrations. It was assumed that the ICG monomers did not degrade during the ICG-MC synthesis. We determined η as

$$\eta = \frac{\text{total mass of ICG in MCs}}{\text{total mass of ICG utilized in synthesis}} \cdot 100 \% \quad (1)$$

2.4 Size Analysis and Morphology Characterization

Particle size analysis was conducted using brightfield and fluorescence microscopy. Small volumes of MCs (<100 μl) suspended in PBS were pipetted onto a glass slide and covered with a coverslip. Scanning electron microscopy was used to characterize the MC morphology.

2.5 Light Sensitivity

Effect of light exposure on ICG absorbance characteristics was analyzed for MCs containing ICG and freely dissolved ICG at room temperature. Preparations were pipetted into 35-mm Petri dishes (5 ml per trial) placed 28 cm directly beneath a broadband 250-W tungsten lamp (Lowel Prolite). Optical power was measured using a Coherent Lasermate 10 power meter with thermal power head. Using an adjustable iris and a collimating lens, the entire dish was illuminated at a uniform intensity of 56 mW/cm^2 . With this intensity and exposure duration, the total energy delivered is comparable to light doses used for photothermal therapy.²⁹ At various time points for up to 2 h, 500 μl was withdrawn from the Petri dish and the absorbance spectrum was recorded. The tempera-

ture of the sample was monitored using a thermometer and never exceeded 28°C. Each experiment was conducted in triplicate.

2.6 Temperature Sensitivity

Preparations of freely dissolved ICG and MCs were aliquotted into microcentrifuge tubes (500 μl per tube) and remained covered in foil. The samples were either refrigerated at 3°C, maintained at room temperature 22°C, or incubated in a water bath at 40°C. Every 24 h, the absorbance spectra for the preparations were recorded and analyzed for up to 96 h. The different temperatures were used to investigate the influence of temperature on the optical stability of ICG. Specifically, incubation at 40°C for several days was used to simulate physiological conditions experienced by nanoparticles as they accumulate at a targeted tumor site following a bolus injection. To determine whether ICG escaped from the MCs over the course of our experiments, the capsules were centrifuged and resuspended in PBS. The absorbance profiles were recorded for both the MCs and the supernatant. Three samples were used for each time point.

2.7 Absorbance Calculations

Alterations in absorbance spectra are a measure of the changes in the concentration of nondegraded ICG molecules as a function of time (t) and wavelength (λ). We use equations reported by Holzer et al. to quantitatively express:

$$\text{abs}_0(\lambda) = c_0 \varepsilon_0(\lambda) l, \quad (2)$$

$$\text{abs}(t, \lambda) = (c_0 - c_d) \varepsilon_0(\lambda) l + c_d \varepsilon_d(\lambda) l, \quad (3)$$

where $\text{abs}_0(\lambda)$ and $\text{abs}(t, \lambda)$ represent the absorbance values immediately after synthesis ($t=0$) and after elapsed time t , respectively, c_0 represents the initial concentration (mol L^{-1}) of nondegraded ICG molecules, c_d represents the concentration (mol L^{-1}) of degraded molecules, $\varepsilon_0(\lambda)$ and $\varepsilon_d(\lambda)$ are the, respective, molar absorptivity ($\text{L mol}^{-1} \text{cm}^{-1}$) of nondegraded and degraded ICG, and l (in centimeters) represents the path length of the sample.¹⁸ From these relationships, the parameter $\zeta(t, \lambda)$ is derived to represent the percent change between the initial and final absorbance spectrum:

$$\zeta(t, \lambda) = \frac{\text{abs}_0(\lambda) - \text{abs}(t, \lambda)}{\text{abs}_0(\lambda)} = \frac{c_d}{c_0} \left(1 - \frac{\varepsilon_d(\lambda)}{\varepsilon_0(\lambda)} \right). \quad (4)$$

The ratio provides a means to evaluate which molecular species, monomers, dimers, or other aggregates within the ICG solutions are most sensitive to light exposure. It is assumed that the degraded molecules have minimal absorption near the monomeric and dimeric peaks of nondegraded ICG molecules^{18,20} [$\varepsilon_d(\lambda) \approx 0$, $\lambda=780$ and 680 nm, respectively].

ICG is useful for various diagnostic and therapeutic applications in its native, monomeric state. Therefore, we are interested in characterizing the potential spectral changes in the absorption peak of ICG monomers at 780 nm that may result from external physical stimuli such as temperature and intense, broadband light exposure, and define the parameter $\phi(t)$ as

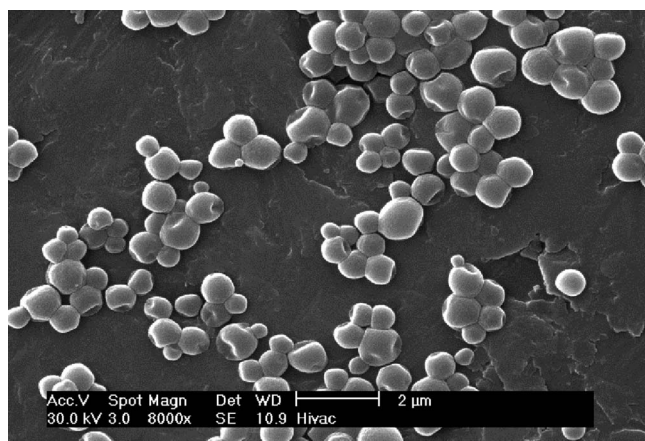


Fig. 1 SEM Image of dextran-coated MCs. Capsules had a spherical conformation and ranged in diameter from 400 to 800 nm.

$$\phi(t) = \frac{\text{abs}(t, \lambda = 780 \text{ nm})}{\text{abs}(t = 0, \lambda = 780 \text{ nm})} \cdot 100 \% . \quad (5)$$

2.8 Degradation Kinetics

The change in absorbance over time was used to determine the kinetics of ICG degradation. As the peak absorbance value was linearly proportional to the ICG concentration within the concentration range used in this study, the decrease in absorbance peak over time was assumed to reflect the physico-chemical transformations of ICG molecules. The degradation processes were assumed to occur in a single step, and degree of linear fits was used to determine the relationship between the degradation rate and the concentration of ICG. Linear fits for $\phi(t)^{-1}$ versus time, $\log_{10}|\phi(t)|$ versus time, and for $\phi(t)$ versus time, were calculated to determine whether the rate of ICG monomer degradation was independent of ICG concentration (zero order), directly proportional to ICG concentration (first order), or proportional to the square of ICG concentration (second order). The reaction order that yielded the best correlation coefficient was considered to be the approximate order.

3 Results

3.1 MC Morphology

Figure 1 shows a scanning electron microscopy (SEM) image of the dextran-coated MCs. The MCs are roughly spherical, and ranged from 400 to 800 nm in diameter. Brightfield and fluorescence microscopy verified that the MCs did not aggregate appreciably in aqueous solution.

3.2 Encapsulation Efficiency and ICG Release Kinetics

Freshly prepared MCs were disintegrated with NaOH, and η was evaluated by comparing the peak absorbance values to a standard curve for ICG dissolved in PBS. Our earlier experiments revealed that η depends largely on the initial ICG concentration and volume utilized in the MC synthesis process. The ICG concentration and volume used for these studies was selected to optimize η , which was determined to range be-

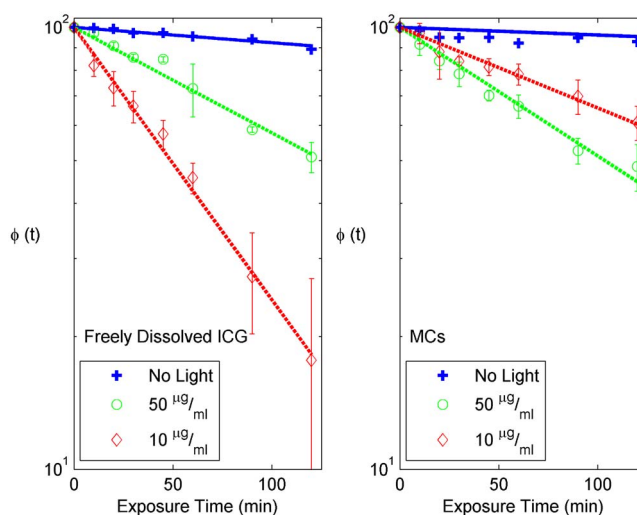


Fig. 2 Influence of broadband light exposure on, $\phi(t)$, normalized monomeric peak absorbance $\text{abs}(\lambda = 780 \text{ nm})$ of freely dissolved ICG (left) and MCs (right) under different exposure conditions. Freely dissolved ICG and ICG within MCs experienced similar amounts of monomeric degradation at $50 \mu\text{g/ml}$. At a more dilute concentration ($10 \mu\text{g/ml}$), ICG monomers within MCs were more stable, while monomers in freely dissolved ICG degraded much more significantly.

tween 48 and 85%. Other experiments showed that when not encapsulated as MCs, PAH, phosphate, and dextran in solution had negligible influence on the absorbance profile of ICG.

The amount of ICG released from the MCs over the course of our studies was determined by absorbance measurements of the supernatants from preparations stored in dark at 3, 22, and 40°C over 2 or 4 days. In the case of MCs stored at 3 and at 22°C , the ICG concentration within the supernatants did not exceed 3% of the initial ICG concentration within the capsules. At 40°C , the supernatant concentration did not exceed 7.5% of the initial capsule concentration. These results suggest that more than 90% of ICG did not escape from the MCs over the course of our experiments. ICG leakage was not considered in the light sensitivity and temperature sensitivity studies. The ICG molecules remain trapped within the aggregate core by electrostatic interaction, and moreover, any change in the absorbance profile at later time points were attributable to the instability of the ICG molecules.

3.3 Light Sensitivity

Figure 2 shows the normalized change in monomeric peak absorbance value, $\phi(t)$, for both MCs and freely dissolved ICG in the dark when irradiated with broadband light for various exposure durations. At a concentration of $50 \mu\text{g/ml}$, freely dissolved ICG was found to degrade significantly in response to broadband light exposure over the course of 2 h. MCs containing a comparable amount of ICG were found to degrade by a similar amount.

As the profiles of $\phi(t)$ versus t yielded the greatest correlation coefficients, the rate of degradation for peak absorbance, and therefore the degradation rate for nondegraded monomeric ICG, followed first-order kinetics. The rate constants were determined by the slope of the linear fits and are

Table 1 Calculated degradation rate constants for freely dissolved ICG and MCs in response to broadband light exposure; all constants have units of inverse minutes.

Influence of Light Exposure and Concentration on ICG Monomer Degradation Rate Constants		
	ICG	MCs
50 $\mu\text{g/ml}$	$k=0.0055$ $R^2=0.9776$	$k=0.0067$ $R^2=0.9683$
10 $\mu\text{g/ml}$	$k=0.0142$ $R^2=0.9928$	$k=0.0042$ $R^2=0.9718$
50 $\mu\text{g/ml}$	$k=0.0008$	$k=0.0008$
(no light exposure)	$R^2=0.9429$	$R^2=0.5372$

provided in Table 1. Interestingly, the degradation rate constants are dramatically different for more dilute preparations (20% of the original concentration) that were irradiated with the same light exposure conditions. When compared to the typical ICG concentrations utilized for this study, the values in Table 1 reveal that the peak absorption value decreases much further for a dilute solution of freely dissolved ICG, with a degradation rate constant nearly 3 times higher than that of the typical solution. This is consistent with previous reports that demonstrate ICG's increased sensitivity to light exposure at lower concentrations.¹⁸ Conversely, a more dilute suspension of MCs demonstrates greater photostability than the more concentrated preparations of MCs and freely dissolved ICG, evident by a more gradual slope. The results suggest that the protection of ICG from photodegradation provided by encapsulation within MCs is concentration dependent, with more dilute capsule preparations allowing greater stability.

Figure 3 shows the $\zeta(t=120 \text{ min}, \lambda)$ profiles for samples that were exposed to broadband light for 120 minutes, the maximum exposure duration. We present results for the wavelength region between 600 and 850 nm, as the absorbance outside this region was essentially negligible both before and after light exposure. In all cases, near maximal change in ζ is found at the monomeric peak, $\lambda=780 \text{ nm}$, indicative of the monomers' sensitivity to light-induced degradation. In the case of freely dissolved ICG at 50 $\mu\text{g/ml}$, the $\zeta(t=120 \text{ min}, \lambda)$ profile exhibits negative values at wavelengths greater than $\lambda=820 \text{ nm}$, suggesting that light exposure for 120 min resulted in increased molar extinction coefficient ϵ in this wavelength region. Other investigators have also reported¹⁸ increased absorbance at wavelengths greater than $\lambda=780 \text{ nm}$ in response to laser light exposure for nearly 1 h. As it is assumed that the degraded ICG molecules have minimal absorbance at the monomeric and dimeric peak for non-degraded ICG, the values of $\zeta(\lambda=780)$ and $\zeta(\lambda=680)$ can be regarded as the fraction of ICG monomers and dimers that degraded over the course of the experiment, respectively. Approximately 83% of the monomers of the freely dissolved ICG in the dilute solution (10 $\mu\text{g/ml}$) degraded, while roughly 50% of the monomers of the freely dissolved ICG

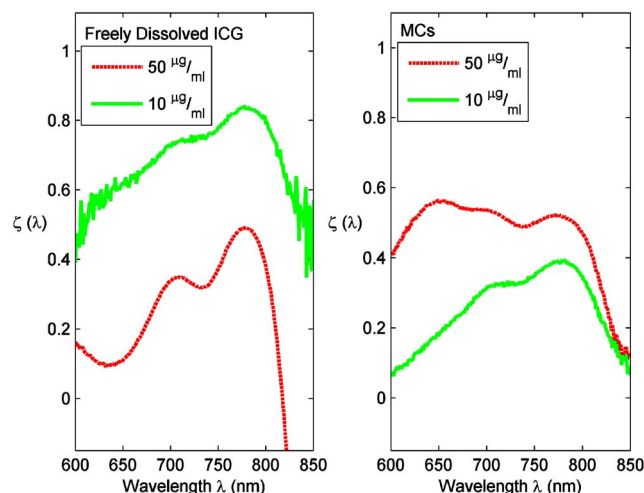


Fig. 3 Spectral absorbance ratio $\zeta(t, \lambda)$ at 2 h of broadband light exposure for freely dissolved ICG (left) and MCs. Freely dissolved ICG degraded more readily at the more dilute concentration (10 $\mu\text{g/ml}$) while the converse was observed in MCs.

and MCs degraded 50 $\mu\text{g/ml}$ concentrations. In the case of the dilute suspension of MCs, 30% of the monomers degraded when exposed to light for 120 min. The freely dissolved ICG samples exhibited dramatic change at the monomeric peak in comparison to the dimeric peak. The flatter profiles of the ICG-MCs suggest that ICG monomers, aggregates, and other oligomer forms of the molecule exhibit comparable sensitivity to light induced degradation.

The $\zeta(t, \lambda)$ values at ($t=48 \text{ min}, \lambda=680 \text{ nm}$) for freely dissolved ICG at concentration of 50 $\mu\text{g/ml}$ shows that approximately 20% of the dimers degraded, whereas nearly 70% of dimers degraded in the case of freely dissolved ICG at concentration of 10 $\mu\text{g/ml}$. The degradation of the monomeric and dimeric molecules resulted in discoloration of freely dissolved ICG at both concentrations. This discoloration was not as pronounced within the MC suspension. For the dilute (10 $\mu\text{g/ml}$) MC suspension, only 26% of the dimers degraded, whereas 54% degraded in the MC suspension 50 $\mu\text{g/ml}$ samples.

3.4 Temperature Sensitivity

To evaluate how encapsulation of ICG within MCs affects ICG sensitivity to temperature, preparations of MCs and freely dissolved ICG at concentration of 50 $\mu\text{g/ml}$ were incubated in the dark at 3, 22, and 40 °C for up to 96 h. Figure 4 displays $\varphi(t)$ at various times for both systems at the three temperatures. In all cases, the correlation coefficients were <0.8 , suggesting that the degradation kinetics did not suitably follow zero-, first-, or second-order trends. Nevertheless, the best-fit profiles for first-order kinetics are included in the figures. Freely dissolved ICG is far more vulnerable to thermal degradation than the ICG within the MCs, as the monomeric peak absorbance decreased by less than 10% for the MCs stored at 40 °C after 48 h. Freely dissolved ICG also experienced noticeable degradation at 22 and 3 °C, whereas virtually no degradation occurred for MCs stored at these temperatures over the course of the experiments.

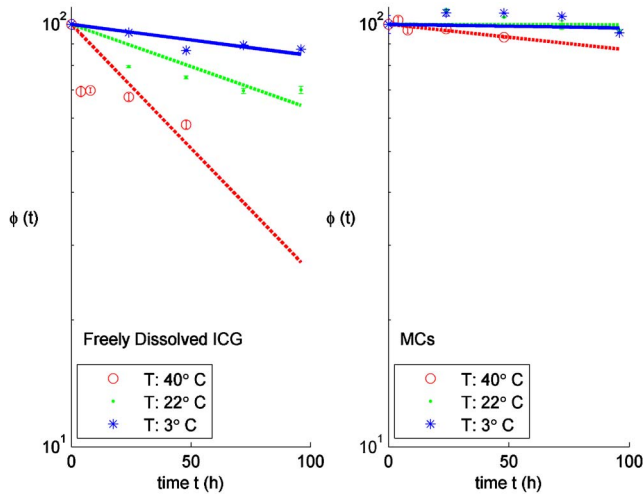


Fig. 4 Influence of temperature on normalized peak absorbance $\phi(t)$ of freely dissolved ICG and MCs.

Figure 5 shows the normalized initial and final absorbance spectra of both freely dissolved ICG and ICG-MCs at 50 $\mu\text{g/ml}$ incubated at 40°C for 48 h. The spectra are normalized by the initial monomeric peak value $\text{abs}(t=0, \lambda = 780 \text{ nm})$. The spectrum for freely dissolved ICG changed dramatically, exhibiting substantially reduced absorbance and broadening at the peak values as well as the emergence of a new, small peak near 850 nm. However, the overall spectrum for the MCs retained the same shape, while the peak values diminished slightly. Similar, but less pronounced, changes in the monomeric and dimeric peaks were observed for the absorbance spectra of freely dissolved ICG incubated at 22 and 3°C, while the spectra for the ICG encapsulated in MCs had little change.

Figure 6 shows $\zeta(t=48 \text{ h}, \lambda)$ at three different temperatures. All of the spectra display large negative values in the

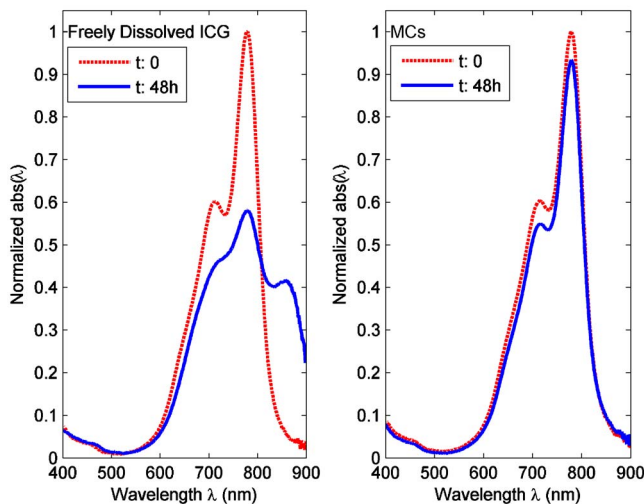


Fig. 5 Absorbance spectra normalized to the monomeric peak ($\lambda = 780 \text{ nm}$) at $t=0$ for both freely dissolved ICG and MCs at 48 h of incubation at 40°C. Baseline profiles prior to incubation at 40°C are also presented for comparison.

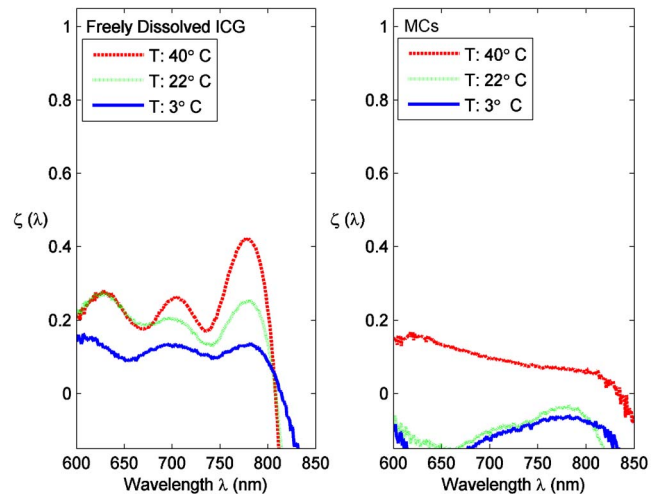


Fig. 6 Spectral absorbance ratios for freely dissolved ICG and MCs, $\zeta(t, \lambda)$, at 48 h of incubation at different temperatures.

NIR region ($\lambda > 800 \text{ nm}$). This might be attributable to the increase in absorbance over time that results from the first stages of J-aggregation. Reports have shown that, at room temperatures, J-aggregation of ICG molecules in solution does not set in for several weeks.²⁰ However, because the initial absorbance in this region is so low ($\ll 1$), even a slight change is emphasized, i.e., normalizing by $\text{abs}_0(\lambda) \ll 1$ yields a more pronounced value for $\zeta(t, \lambda)$. With increasing temperature, ICG solution is more prone to degradation, as indicated by the higher values for $\zeta(\lambda)$. The maximal change for freely dissolved ICG occurs at the monomeric peak ($\lambda = 780 \text{ nm}$), indicating that the monomers degraded by 13, 25, and 42% when stored at 3, 22, and 40°C, respectively. ICG dimers also experience noticeable degradation, by as much as 12, 19, and 20% after being stored at 3, 22, and 40°C, respectively. The high values near $\lambda = 680 \text{ nm}$ indicate the degradation of dimers, although the actual local maximum occurs closer to 705 nm.

For the MCs, the maximal change in absorbance occurs around the dimeric peak in the samples stored at 3 and 22°C. The negative $\zeta(t=48 \text{ h}, \lambda = 680 \text{ nm})$ values of -13 and -15% suggest that more dimers are present after incubation at 22 and 3°C, respectively. At these temperatures, a slight negative change is also observed at the monomeric peak, however, the change is negligible and most likely a consequence of experimental error. For the sample stored at 40°C, the wavelengths at which there is the most pronounced change in absorbance occurs between 620 and 640 nm, with a steady decline in sensitivity at higher wavelengths. At all three temperatures, $\zeta(\lambda)$ is significantly lower for the MCs than for freely dissolved ICG stored under the same conditions. At all temperatures, less than 7% of the ICG monomers located within the MCs underwent degradation.

4 Discussion

Dextran-coated electrostatically assembled MCs with diameters ranging from 400 to 800 nm and containing ICG were synthesized with η ranging between 48 and 85%. Synthesis parameters were selected to yield MCs with maximal η val-

ues and smallest capsule diameter. Both η and MC diameter depend largely on the initial ICG concentration and volume utilized in the synthesis process. Adding smaller amounts of concentrated ICG solution resulted in clumping of the polymer cores and therefore influenced the size of the MCs, while adding large volumes of more dilute ICG solution influenced the R ratio of positive polymer to dissociated salt anions and resulted in smaller cores. The polymer aggregate core of the complex has a finite number of positive charges for ICG to bind to, which establishes a maximal limit for the number of ICG molecules that can be incorporated into each capsule.

Encapsulating ICG molecules within MCs enables protection of the molecules from light-induced degradation only under certain conditions. The photostability of the complexes is dependent on their concentration. ICG monomers within the MCs remain resistant to degradation when the MCs are suspended in a larger volume of liquid (i.e., less dilute suspension of MCs). This is in contrast to freely dissolved ICG, whose stability decreases drastically in more dilute solutions.

Our results show that entrapment within the MCs effectively protects ICG monomers from thermal degradation. The exposure to high temperatures causes a significant reduction in the absorbance of freely dissolved ICG at its monomeric and dimeric peaks, indicative of their degradation. At each temperature tested, the absorbance profile for the capsules at the final time shows a slight increase in absorbance at wavelength range from $\lambda=800$ to 900 nm, as seen for $T=40^\circ\text{C}$ in Fig. 5. This could possibly indicate the temperature-independent onset of a molecular transformation such as J-aggregation within the MCs. Figure 6 also shows that a third constituent is prone to thermally induced changes for freely dissolved ICG stored at room temperature or warmer conditions. The molecule, which absorbs light between $\lambda=600$ to 650 nm, is most likely a more aggregated oligomer or possibly an unstable leucoform. The molecule is either not present in the ICG solution stored at 4°C , or it does not undergo any changes at this colder temperature. These phenomena must be further investigated. In Figs. 3 and 5, the large decrease of $\zeta(t, \lambda)$ in the IR region ($\lambda > 780$ nm) for ICG solution reflect an increase in the absorbance value within this wavelength region. This could have emerged through charge transfer with ambient O_2 molecules, or it could indicate the formation of other photoproducts or aggregates that absorb light in the long-wavelength range.

Photodegradation comes about from the electronic excitation of ICG molecules to a higher singlet or triplet energy state. The change in energy states can lead to a change in conformational state of the molecules, vibrational excitation, or slight heat generation from nonradiative relaxation. Any of these effects can lead to the formation of destructive radical species. Thermally mediated molecular degradation is attributable to the increased likelihood of vibrational and translational agitation, which also increases the prospect of radical formation or the diffusion of intrinsic solvent radicals within the solvent to vulnerable molecular sites.³⁰

From our thermal stability results, it can be reasoned that, when encapsulated within the complexes, the mobility of ICG is significantly hindered by its charge interactions within the polymer-salt core. The electrostatic attraction immobilizes the molecules sufficiently enough to render them invulnerable to

random changes in vibrational and translational states that occur at elevated temperatures. However, when the ICG molecules absorb photons of light, the excited molecule has sufficient energy to overcome the immobilizing electrostatic effect, and altered vibrational state and subsequent radical formation within the molecules can ensue. While, the effect of concentration on photostability must be further investigated, we presume that the effect could be explained by the density of ICG molecules and the amount of destructive radicals generated in response to light. In a more concentrated collection of capsules, the excited ICG molecules are more densely packed, and radicals generated from photo-excited molecules will have a more pronounced effect on nearby ICG molecules. A greater population of excited ICG molecules undergoing nonradiative relaxation also leads to a larger rise in temperature, which would more likely degrade the neighboring, vulnerable photoexcited ICG molecules. The same effect would not be found in more concentrated solutions of freely dissolved ICG, as they are more likely to produce aggregates and oligomers with different absorbance peaks.

The discoloration and diminished absorbance of ICG at its NIR peak is attributable in part to fragmentation of molecules, but it is primarily the result of loss of conjugated double bonds within molecules that otherwise remain intact. Encapsulation within MCs reduces the likelihood of these molecular changes by immobilizing the molecules through electrostatic attraction to the positive charges distributed throughout the core.

As the absorbance properties of ICG are not adversely affected through encapsulation within the MCs, the dextran-coated MCs containing ICG could be useful for photothermal therapy. The MCs can be used to overcome drawbacks that limit the ICG therapeutic abilities, including rapid clearance from the bloodstream and its inability to be localized. By functionalizing the dextran surface with site-specific antibodies, the MCs could provide an efficient means to deliver and localize ICG to targeted therapeutic sites such as tumors.

5 Conclusion

ICG was encapsulated within spherical dextran-coated MCs with diameters ranging from 400 to 800 nm, and the sensitivity of the encapsulated ICG to broadband light and temperature was investigated. We found that the sensitivity of encapsulated ICG to light varies with the concentration of ICG incorporated within the MCs. Encapsulation of ICG within MCs reduces the effects of thermally induced degradation.

Acknowledgments

This work was supported by a grant from the National Institutes of Health under Grant No. GMO 8362. We thank Dr. Parmeswaran Diagaradjane for several helpful discussions.

References

1. M. L. J. Landsman, G. Kwant, G. A. Mook, and W. G. Zijlstra, "Light-absorbing properties, stability, and spectral stabilization of indocyanine green," *J. Appl. Physiol.* **40**, 575–583 (1976).
2. S. A. Prahl, "Optical absorption properties of indocyanine green (ICG)," available at <http://omlc.org/spectra/icg/index.html>, accessed on December 15, 2006.
3. J. G. Webster, "Measurement of flow and volume of blood," in *Medical Instrumentation: Application and Design*, G. Webster, Ed., Wiley,

- New York (1998).
4. R. C. Benson and H. A. Kues, "Fluorescence properties of indocyanine green as related to angiography," *Phys. Med. Biol.* **23**, 159–163 (1978).
 5. V. Ntziachristos, A. G. Yodh, M. Schnall, and B. Chance, "Concurrent MRI and diffuse optical tomography of breast after indocyanine green enhancement," *Proc. Natl. Acad. Sci. U.S.A.* **97**, 2767–2772 (2000).
 6. A. Rübber, S. Eren, R. Krein, H. Younoussi, U. Böhler, and V. Wientert, "Infrared videoangiography of the skin with indocyanine green—rat random cutaneous flap model and results in man," *Microvasc. Res.* **47**, 240–251 (1994).
 7. L. S. Bass, N. Moazami, J. Pocsidio, M. C. Oz, P. LoGerfo, and M. R. Treat, "Changes in type I collagen following laser welding," *Lasers Surg. Med.* **12**, 500–505 (1992).
 8. S. Fickweiler, R. M. Szeimies, W. Bäuml, P. Steinbach, S. Karrer, A. E. Goetz, C. Abels, F. Hofstädter, and M. Landthaler, "Indocyanine green: intracellular uptake and phototherapeutic effects in vitro," *J. Photochem. Photobiol., B* **38**, 178–183 (1997).
 9. C. Abels, S. Fickweiler, P. Weiderer, W. Bäuml, F. Hofstädter, M. Landthaler, and R. M. Szeimies, "Indocyanine green (ICG) and laser irradiation induce photooxidation," *Arch. Dermatol. Res.* **292**, 404–411 (2000).
 10. W. R. Chen, R. L. Adams, A. K. Higgins, K. E. Bartels, and R. E. Nordquist, "Photothermal effects on murine mammary tumors using indocyanine green and 808-nm diode laser: an in-vivo efficacy study," *Cancer Lett.* **98**, 169–173 (1995).
 11. W. Bäuml, C. Abels, S. Karrer, T. Weiß, H. Messmann, M. Landthaler, and R. M. Szeimies, "Photooxidative killing of human colonic cancer cells using indocyanine green and infrared light," *Br. J. Cancer* **80**, 360–363 (1999).
 12. K. Urbanska, B. Romnaowska-Dixon, Z. Matuszak, J. Oszejca, P. Nowak-Sliwinska, and G. Stochel, "Indocyanine green as a prospective sensitizer for photodynamic therapy of melanomas," *Acta Biochim. Pol.* **49**, 387–391 (2002).
 13. C. Abels, S. Karrer, W. Bäuml, A. E. Goetz, M. Landthaler, and R. M. Szeimies, "Indocyanine green and laser light for the treatment of AIDS-associated cutaneous Kaposi's sarcoma," *Br. J. Cancer* **77**, 1021–1024 (1998).
 14. V. V. Tuchin, E. A. Genina, A. N. Bashkatov, G. V. Simonenko, O. D. Odoevskaya, and G. B. Altshuler, "A pilot study of ICG laser therapy of acne vulgaris: photodynamic and photothermolysis treatment," *Lasers Surg. Med.* **33**, 296–310 (2003).
 15. A. J. Welch, M. J. C. V. Gemert, W. M. Star, and B. C. Wilson, "Definitions and overview of tissue optics," in *Optical-Thermal Response of Laser Irradiated Tissue*, A. J. Welch, M. J. C. V. Gemert, and Kogelnik, Eds., pp. 15–46, Plenum, New York (1995).
 16. M. A. Yaseen, P. Diagaradjane, B. M. Pikkula, J. Yu, M. S. Wong, and B. Anvari, "Photothermal and photochemical effects of laser light absorption by indocyanine green (ICG)," *Proc. SPIE* **5965**, 27–35 (2005).
 17. T. Desmettre, J. M. Devoisselle, and S. Mordon, "Fluorescence properties and metabolic features of indocyanine green (ICG) as related to angiography," *Surv. Ophthalmol.* **45**, 15–27 (2000).
 18. W. Holzer, M. Maurer, A. Penzkofer, R. M. Szeimies, C. Abels, M. Landthaler, and W. Bäuml, "Photostability and thermal stability of indocyanine green," *J. Photochem. Photobiol., B* **47**, 155–164 (1998).
 19. O. G. Bjornsson, R. Murphy, and V. S. Chadwick, "Physicochemical studies of indocyanine green (ICG): absorbance/concentration relationship, pH tolerance and assay precision in various solvents," *Experientia* **38**, 1441–1442 (1982).
 20. M. Maurer, A. Penzkofer, and J. Zweck, "Dimerization, J-aggregation and J-disaggregation dynamics of indocyanine green in heavy water," *J. Photochem. Photobiol., B* **47**, 68–73 (1998).
 21. R. Philip, A. Penzkofer, W. Bäuml, R. M. Szeimies, and C. Abels, "Absorption and fluorescence spectroscopic investigation of indocyanine green," *J. Photochem. Photobiol., A* **96**, 137–148 (1996).
 22. V. Saxena, M. Sadoqi, and J. Shao, "Degradation kinetics of indocyanine green in aqueous solution," *J. Pharm. Sci.* **92**, 2090–2097 (2003).
 23. S. Mordon, J. M. Devoisselle, S. Begu, and T. Desmettre, "Laser-induced release of liposome-encapsulated dye: a new diagnostic tool," *Lasers Med. Sci.* **13**, 181–188 (1998).
 24. T. J. Desmettre, S. Soulie-Begu, J. M. Devoisselle, and S. R. Mordon, "Diode laser-induced thermal damage evaluation on the retina with a liposome dye system," *Lasers Surg. Med.* **24**, 61–68 (1999).
 25. V. Saxena, M. Sadoqi, and J. Shao, "Enhanced photo-stability, thermal-stability and aqueous-stability of indocyanine green in polymeric nanoparticulate systems," *J. Photochem. Photobiol., B* **74**, 29–38 (2004).
 26. J. Yu, M. A. Yaseen, B. Anvari, and M. S. Wong, "Synthesis of near-infrared absorbing nanoparticle-assembled complexes," *Chem. Mater.* **19**, 1277–1284 (2007).
 27. R. K. Rana, V. S. Murthy, J. Yu, and M. S. Wong, "Nanoparticle self-assembly of hierarchically ordered microcapsule structures," *Adv. Mater. (Weinheim, Ger.)* **17**, 1145–1150 (2005).
 28. T. Heinze, T. Liebert, B. Heublein, and S. Hornig, "Functional polymers based on dextran," *Adv. Polym. Sci.* **205**, 199–291 (2006).
 29. M. H. Niemz, "Thermal interaction," in *Laser-Tissue Interactions: Fundamentals and Applications*, pp. 58–85, Springer-Verlag, Berlin (1996).
 30. J. F. Rabek, *Photodegradation of Polymers: Physical Characteristics and Applications*, Springer, Berlin (1996).